



AFRL-RY-WP-TP-2008-1153

**CONSTRAINED ESTIMATION FOR GPS/DIGITAL MAP
INTEGRATION (POSTPRINT)**

Mikel Miller, Erik Blasch, Thao Nguyen, and Chun Yang
Sigtem Technology, Inc.

JANUARY 2007

Approved for public release; distribution unlimited.

See additional restrictions described on inside pages

STINFO COPY

**AIR FORCE RESEARCH LABORATORY
SENSORS DIRECTORATE
WRIGHT-PATTERSON AIR FORCE BASE, OH 45433-7320
AIR FORCE MATERIEL COMMAND
UNITED STATES AIR FORCE**

REPORT DOCUMENTATION PAGE				<i>Form Approved</i> OMB No. 0704-0188	
<p>The public reporting burden for this collection of information is estimated to average 1 hour per response, including the time for reviewing instructions, searching existing data sources, gathering and maintaining the data needed, and completing and reviewing the collection of information. Send comments regarding this burden estimate or any other aspect of this collection of information, including suggestions for reducing this burden, to Department of Defense, Washington Headquarters Services, Directorate for Information Operations and Reports (0704-0188), 1215 Jefferson Davis Highway, Suite 1204, Arlington, VA 22202-4302. Respondents should be aware that notwithstanding any other provision of law, no person shall be subject to any penalty for failing to comply with a collection of information if it does not display a currently valid OMB control number. PLEASE DO NOT RETURN YOUR FORM TO THE ABOVE ADDRESS.</p>					
1. REPORT DATE (DD-MM-YY) January 2007		2. REPORT TYPE Conference Paper Postprint		3. DATES COVERED (From - To) 08 April 2005 – 08 September 2006	
4. TITLE AND SUBTITLE CONSTRAINED ESTIMATION FOR GPS/DIGITAL MAP INTEGRATION (POSTPRINT)				5a. CONTRACT NUMBER FA8650-05-C-1828	
				5b. GRANT NUMBER	
				5c. PROGRAM ELEMENT NUMBER 65502F	
6. AUTHOR(S) Mikel Miller and Thao Nguyen (AFRL/RYRN) Erik Blasch (AFRL/RYAA) Chun Yang (Sigtem Technology, Inc.)				5d. PROJECT NUMBER 3005	
				5e. TASK NUMBER 13	
				5f. WORK UNIT NUMBER 300513CY	
7. PERFORMING ORGANIZATION NAME(S) AND ADDRESS(ES) Reference Systems Branch (AFRL/RYRN) RF Sensor Technology Division Assessment and Integration Branch (AFRL/RYAA) Sensor ATR Technology Division Air Force Research Laboratory, Sensors Directorate Wright-Patterson Air Force Base, OH 45433-7320 Air Force Materiel Command, United States Air Force				8. PERFORMING ORGANIZATION REPORT NUMBER Sigtem Technology, Inc. 1343 Parrott Drive San Mateo, CA 94402-3630	
9. SPONSORING/MONITORING AGENCY NAME(S) AND ADDRESS(ES) Air Force Research Laboratory Sensors Directorate Wright-Patterson Air Force Base, OH 45433-7320 Air Force Materiel Command United States Air Force				10. SPONSORING/MONITORING AGENCY ACRONYM(S) AFRL/RYRN	
				11. SPONSORING/MONITORING AGENCY REPORT NUMBER(S) AFRL-RY-WP-TP-2008-1153	
12. DISTRIBUTION/AVAILABILITY STATEMENT Approved for public release; distribution unlimited.					
13. SUPPLEMENTARY NOTES Paper produced under contract FA8650-05-C-1828 for technical report AFRL-RY-WP-TR-2008-1137, SOFTWARE TOOLKIT FOR NONLINEAR FILTERS FOR GLOBAL POSITIONING SYSTEM (GPS) OPERATIONAL CONTROL SEGMENT (OCS) ESTIMATION AND OTHER APPLICATIONS. Conference paper published in the Proceedings of the IEEE Institute of Navigation, National Technical Meeting, Vol. 2, NTM 2007 (held Jan 22-24 2007, San Diego, CA; Publisher: Institute of Navigation). The U.S. Government is joint author of this work and has the right to use, modify, reproduce, release, perform, display, or disclose the work. PAO Case Number: SN 06-0401; Clearance date: 20 Dec 2006. Paper contains color.					
14. ABSTRACT Linear and nonlinear constrained estimation is investigated in this paper as an optimal method to integrate GPS fixes with digital maps so as to improve accuracy and reliability. In addition to emergency location and roadside assistance, the integration of GPS with digital maps becomes an increasingly popular application in automobiles particularly for real-time routing, driving guidance, and street prompting. A position fix is obtained by a GPS receiver, which may be subject to significant errors in urban canyons due to such effects as multipath and weak signal, whereas a digital map provides the road network of a region in which a user is traveling. <p style="text-align: right;"><i>Abstract concludes on reverse side →</i></p>					
15. SUBJECT TERMS					
16. SECURITY CLASSIFICATION OF:			17. LIMITATION OF ABSTRACT: SAR	18. NUMBER OF PAGES 16	19a. NAME OF RESPONSIBLE PERSON (Monitor) Thao Nguyen
a. REPORT Unclassified	b. ABSTRACT Unclassified	c. THIS PAGE Unclassified			

14. ABSTRACT (concluded)

When the information about roads is as accurate as (or even better than) GPS measurements, it is desired naturally to incorporate such information into position solution. In this paper, roads are modeled with analytic functions and its integration (fusion) with a GPS position fix is cast as linear and/or non-linear state constraints in an optimization procedure. Similarly, the velocity estimates and the road directions are treated as another pair of constraints. The constrained optimization is then solved with the Lagrangian multiplier, leading to a closed-form solution for linear constraints and an iterative solution for nonlinear constraints. Geometric interpretations of the solutions are provided for simple cases. Computer simulation results are presented to illustrate the algorithms.

Constrained Estimation For GPS/Digital Map Integration

Mikel Miller Erik Blasch
Air Force Research Lab/RYRN Air Force Research Lab/RYAA

Thao Nguyen Chun Yang
Air Force Research Lab/RYRN Sigtem Technology, Inc.

BIOGRAPHIES

Dr. Mikel Miller is the Technical Advisor for the Reference Systems Branch, Sensors Directorate, Air Force Research Laboratory, WPAFB, OH. He received his Ph.D. in Electrical Engineering from the Air Force Institute of Technology (AFIT), WPAFB, Ohio, in 1998. Since 1986, he has focused on navigation system R&D related to GPS, GPS/INS integrations, alternative navigation techniques including bio-inspired navigation and signals of opportunity based navigation, autonomous vehicle navigation and control, and multi-sensor fusion. He is currently responsible for both in-house and contracted R&D projects advancing navigation technology. He is also an Adjunct Professor of EE at AFIT and Miami University of Ohio. Dr. Miller is a member of the ION, RIN, IEEE, and AIAA.

Dr. Erik Blasch is a Fusion Evaluation Tech Lead for the Assessment & Integration Branch, Sensors Directorate, Air Force Research Laboratory, WPAFB, OH. He is an adjunct professor at Wright State University (WSU)/University of Dayton (UD)/AFIT and a Reserve Major at the Air Force Office of Scientific Research (AFOSR). He received his Ph.D. in Electrical Engineering from WSU in 1999, a MSEE from WSU in 1997, a MSME from Georgia Tech in 1994, and a BSME from MIT in 1992 among other advanced degrees in engineering, health science, economics, and business administration. He is the President of the International Society of Information Fusion (ISIF) and active in IEEE, SPIE, and ION. His research interests include target tracking, sensor fusion, automatic target recognition, biologically-inspired robotics, and controls.

Thao Nguyen is a Ph.D. candidate in the Electrical and Computer Engineering Department at the Air Force Institute of Technology (AFIT), Wright-Patterson AFB, Ohio. He also works as an Electronics Engineer at the Reference Systems Branch, Sensors Directorate, Air

Force Research Laboratory, WPAFB, OH. Mr. Nguyen has been involved with navigation-related research, development, and test since 2002 and his current areas of interest include high anti-jamming technologies for GPS receivers, GPS/INS integration, multi-sensor fusion, and personal navigation using signals of opportunity (SoOP).

Dr. Chun Yang received his title of Docteur en Science from the Université de Paris (No. XI, Orsay), France, in 1989. After two years of post-doctoral research at the University of Connecticut, he moved on with his industrial R&D career. Since 1993, he has been with Sigtem Technology, Inc. and has been working on numerous GPS, integrated inertial, and adaptive array related projects.

ABSTRACT

Linear and nonlinear constrained estimation is investigated in this paper as an optimal method to integrate GPS fixes with digital maps so as to improve accuracy and reliability. In addition to emergency location and roadside assistance, the integration of GPS with digital maps becomes an increasingly popular application in automobiles particularly for real-time routing, driving guidance, and street prompting. A position fix is obtained by a GPS receiver, which may be subject to significant errors in urban canyons due to such effects as multipath and weak signal, whereas a digital map provides the road network of a region in which a user is traveling. When the information about roads is as accurate as (or even better than) GPS measurements, it is desired naturally to incorporate such information into position solution. In this paper, roads are modeled with analytic functions and its integration (fusion) with a GPS position fix is cast as linear and/or nonlinear state constraints in an optimization procedure. Similarly, the velocity estimates and the road directions are treated as another pair of constraints. The constrained optimization is then solved with the

Lagrangian multiplier, leading to a closed-form solution for linear constraints and an iterative solution for nonlinear constraints. Geometric interpretations of the solutions are provided for simple cases. Computer simulation results are presented to illustrate the algorithms.

INTRODUCTION

With the rapid build up of the geographic information system (GIS) including digital road maps (DRM) and digital terrain elevation database (DTED), information about roads is becoming more accurate, up to date, and more accessible. The best route to a destination can be easily found on the internet. Road and terrain information has been used in the past for navigation via terrain contour matching. An increasingly popular use of digital maps is for automobile navigation with a GPS receiver [Bullock et al., 2006].

This paper is concerned with improving the kinematic state (position and velocity) of a user vehicle via integrating (or fusing) its GPS fixes with the information about a road along which the vehicle is believed to be traveling. When the information about roads is as accurate as (or even better than) GPS measurements, it is desirable to incorporate such information (fusion) into an integrated solution. When a vehicle travels off-road or on an unknown road, the state estimation problem is unconstrained. However, when the vehicle is traveling on a known road, be it straight or curved, the state estimation problem can be cast as constrained with the road network information available from digital road/terrain maps. Without making full use of this additional information about the state constraints, the state estimates, even obtained with the Kalman filter, cannot be truly optimal.

To use such state constraints, previous attempts can be put into several groups. The first group is to incorporate road information into the state estimation process. One technique is to reduce the system model parameterization. Another technique is to translate the state constraints onto the state process and/or observation noise covariance matrix for the estimation filter [Kirubarajan et al., 2000]. Yet another technique is to project a dynamic system onto linear state constraints and then apply the Kalman filter to the projected systems [Ko and Bitmead, 2006]. Similarly, for nonlinear state constraints, there is the one-dimensional (1D) representation of a target motion along a curvilinear road [Yang, Bakich, Blasch, 2005]. The technique to model bounded random variables with truncated densities also belongs to this group, which could easily work with nonlinear filters such as a particle filter [Ristic, Arullampalam, and Gordon, 2004].

The second group is to treat state constraints as perfect (pseudo) measurements. For a road segment, its analytic model not only constrains the target position but also the

direction of the velocity vector. Indeed, the velocity vector is closely aligned with the road orientation for a linear segment and with the tangent vector at the vehicle position for a nonlinear segment. Furthermore, an estimate of centripetal acceleration can be obtained given the curvature and the vehicle speed.

In the third group, an unconstrained Kalman filter solution is first obtained and then the unconstrained state estimate is projected onto the constrained surface. This technique can also be viewed as post-processing (estimation or updating) correction [Simon, and Chia, 2002], track to road fusion [Yang and Blasch, 2006], or GPS and map integration referred to as in this paper. In conventional track fusion, two or more tracks are available, each consisting of an estimate of the underlying track with its estimation error covariance. The fused track is typically found that minimizes the sum of covariance-weighted state errors squared [Bar-Shalom and Li, 1995; Blackman and Popoli, 1999]. In contrast to this conventional track fusion that operates on individual state values (points), fusion with road involves a state value (a point) and a subset of state values (an interval). In this paper, roads are modeled with analytic functions and its fusion with a GPS fix is therefore formulated as linear or nonlinear state constraints in an optimization procedure.

In this paper, the constrained optimization is solved with the Lagrangian multiplier, leading to a closed-form solution for linear constraints and an iterative solution for nonlinear constraints. In the latter case, we present a method that allows for the use of second-order nonlinear state constraints. The method can provide better approximation to higher order nonlinearities. The new method is based on a computational algorithm that iteratively finds the Lagrangian multiplier. The use of a second-order constraint vs. linearization is a tradeoff between reducing approximation errors to higher-order nonlinearities and keeping the problem computationally tractable.

The GPS/map integration considered in this map is a “point” operation in the sense that each GPS fix is updated onto a road. It is possible to implement an “interval” operation in which a sequence of GPS fixes (e.g., angular turns vs. distance traveled) can be compared with a digital road map. Another way to use map information to improve navigation in a stop-go urban environment is to perform map-predictive model selection and updating. These and other aspects will be addressed in a future paper.

TRACK FUSION WITH LINEAR SEGMENTS

When a road segment is straight, it can be modeled as a linear state constraint. In this section, we first summarize the results for linearly constrained state estimation [Simon and Chia, 2002] as an approach to GPS integration with

linear road segments. We then show that this linearly constrained state estimation is equivalent to use of constraints as measurements in state update. Finally, we provide a simple geometric interpretation of the linearly constrained state estimation.

Linearly Constrained State Estimation

Consider a linear time-invariant discrete-time dynamic system together with its measurement as

$$\underline{x}_{k+1} = A\underline{x}_k + B\underline{u}_k + \underline{w}_k \quad (1a)$$

$$\underline{y}_k = C\underline{x}_k + \underline{v}_k \quad (1b)$$

where the underscore indicates a vector quantity, the subscript k is the time index, \underline{x} is the state vector, \underline{u} is a known input, \underline{y} is the measurement, and \underline{w} and \underline{v} are state and measurement noise processes, respectively. It is implied that all vectors and matrices have compatible dimensions, which are omitted for simplicity.

The goal is to find an estimate denoted by $\hat{\underline{x}}_k$ of \underline{x}_k given the measurements up to time k denoted by $Y_k = \{\underline{y}_0, \dots, \underline{y}_k\}$. Under the assumptions that the state and measurement noises are uncorrelated zero-mean white Gaussian with $\underline{w} \sim \mathcal{N}\{0, Q\}$ and $\underline{v} \sim \mathcal{N}\{0, R\}$ where Q and R are positive semi-definite covariance matrices, the Kalman filter provides an optimal estimator in the form of $\hat{\underline{x}}_k = E\{\underline{x}_k | Y_k\}$ [Anderson and Moore, 1979]. Starting from an initial estimate $\hat{\underline{x}}_0 = E\{\underline{x}_0\}$ and its estimation error covariance matrix $P_0 = E\{(\underline{x}_0 - \hat{\underline{x}}_0)(\underline{x}_0 - \hat{\underline{x}}_0)^T\}$ where the superscript T stands for matrix transpose, the Kalman filter equations specify the propagation of $\hat{\underline{x}}_k$ and P_k over time and the update of $\hat{\underline{x}}_k$ and P_k by measurement \underline{y}_k as

$$\bar{\underline{x}}_{k+1} = A\hat{\underline{x}}_k + B\underline{u}_k \quad (2a)$$

$$\bar{P}_{k+1} = AP_k A^T + Q \quad (2b)$$

$$\hat{\underline{x}}_{k+1} = \bar{\underline{x}}_{k+1} + K_{k+1}(\underline{y}_{k+1} - C\bar{\underline{x}}_{k+1}) \quad (2c)$$

$$P_{k+1} = (I - K_{k+1}C)\bar{P}_{k+1} \quad (2d)$$

$$K_{k+1} = \bar{P}_{k+1}C^T(CP_{k+1}C^T + R)^{-1} \quad (2e)$$

where $\bar{\underline{x}}_{k+1}$ and \bar{P}_{k+1} are the predicted state and prediction error covariance, respectively.

Now in addition to the dynamic system of (1), we are given the linear state constraint equation

$$D\underline{x}_k = \underline{d} \quad (3)$$

where D is a known constant matrix of full rank and \underline{d} is a known vector. The number of rows in D is the number of constraints, which is assumed to be less than the number of states. If D is a square matrix, the state is fully constrained and thus can be solved by inverting (3). Although no time index is given to D and \underline{d} in (3), it is

implied that they can be time-dependent, leading to piecewise linear constraints.

The constrained Kalman filter according to [Simon and Chia, 2002] is constructed by directly projecting the unconstrained state estimate $\hat{\underline{x}}_k$ onto the constrained surface $\mathcal{S} = \{\underline{x}: D\underline{x} = \underline{d}\}$. It is formulated as the solution to the problem

$$\bar{\underline{x}} = \arg \min_{\underline{x} \in \mathcal{S}} (\underline{x} - \hat{\underline{x}})^T W (\underline{x} - \hat{\underline{x}}) \quad (4)$$

where W is a symmetric positive definite weighting matrix.

Based on the Lagrangian multiplier technique, the solution to the constrained optimization in (4) is given by

$$\bar{\underline{x}} = \hat{\underline{x}} - W^{-1}D^T(DW^{-1}D^T)^{-1}(D\hat{\underline{x}} - \underline{d}) \quad (5)$$

Several interesting statistical properties of the constrained Kalman filter are presented in [Simon and Chia, 2002]. This includes the fact that the constrained state estimate as given by (5) is an unbiased state estimate for the system in (1) subject to the constraint in (3) for a known symmetric positive definite weighting matrix W . Furthermore when $W = P^{-1}$, the constrained state estimate has a smaller error covariance than that of the unconstrained state estimate, and it is actually the smallest for all constrained Kalman filters of this type. Similar results hold in terms of the trace of the estimation error covariance matrix when $W = I$.

Linear Road Constraint as Pseudo Measurement

As described above, the linear constrained estimator (5) can be obtained by different methods. It is shown in this section that it is also equivalent to the solution where the linear state constraints are considered as perfect (pseudo) measurements.

For the linear time-invariant discrete-time dynamic system (1a) and its measurement (1b), consider the linear state constraint (3) as another measurement to the system, which can be used to perform the filter measurement update (2c) and (2d) right after (1b) without the filter time propagation (2a) and (2b) (i.e., stay the same). To apply (2), we identify the following equivalence:

$$A = I, B = 0; Q = 0 \quad (6a)$$

$$C = D, R = 0, \underline{y}_k = \underline{d} \quad (6b)$$

Given the unconstrained solution $(\hat{\underline{x}}_k, P_k)$, the prediction step is given by (2a) and (2b):

$$\bar{\underline{x}}_{k+1} = \hat{\underline{x}}_k \quad (7a)$$

$$\bar{P}_{k+1} = P_k \quad (7b)$$

The Kalman filter gain is given by:

$$K_{k+1} = P_k D^T (D P_k D^T)^{-1} \quad (8)$$

The updated state and error covariance becomes

$$\hat{\underline{x}}_{k+1} = \hat{\underline{x}}_k + P_k D^T (D P_k D^T)^{-1} (\underline{d} - D \hat{\underline{x}}_k) \quad (9a)$$

$$P_{k+1} = P_k - P_k D^T (D P_k D^T)^{-1} D P_k \quad (9b)$$

If we choose $W = P_k^{-1}$, (9a) becomes

$$\hat{\underline{x}}_{k+1} = \hat{\underline{x}}_k + W^{-1} D^T (D W^{-1} D^T)^{-1} (\underline{d} - D \hat{\underline{x}}_k) \quad (10a)$$

$$= \hat{\underline{x}}_k - W^{-1} D^T (D W^{-1} D^T)^{-1} (D \hat{\underline{x}}_k - \underline{d}) \quad (10b)$$

which is exactly the same as the solution given by (5).

Geometric Interpretation

It is proved in [Yang and Blasch, 2006] that the linear constrained estimation is the orthogonal projection of the unconstrained estimate onto the constrained surface. It provides a theoretical justification of the intuitive practice of finding a point along the road that is of the shortest distance. The result thus complements [Simon and Chia, 2002], providing an interesting geometrical interpretation to the linear constrained estimation by estimate projection.

TRACK FUSION WITH NONLINEAR SEGMENTS

When a road segment is curved, it can be modeled as a nonlinear state constraint. In this section, we first analyze the linearizing approach and the associated constraint approximation error. We then present an iterative solution to a second order state constraint. Finally, we offer a geometric interpretation of a solution under a circular constraint and a simple approach to a more general second order state constraint.

Approximation Errors in Constraint Linearization

To deal with nonlinearity, a simple approach is to project the unconstrained state estimate onto linearized state constraints. Once the constraints are linearized, the results presented in the previous section for linear cases can be applied. However, linearization introduces constraint approximation error, which is a function of the nonlinearity and, more importantly, of the point around which the linearization takes place. This may lead to an undesired divergence problem as analyzed below.

Consider the nonlinear state constraint of the form

$$g(\underline{x}) = \underline{h} \quad (11)$$

We can expand the nonlinear state constraints about a constrained state estimate $\tilde{\underline{x}}$ and for the i^{th} row of (11), we have

$$g_i(\underline{x}) - h_i = g_i(\tilde{\underline{x}}) + g_i'(\tilde{\underline{x}})^T (\underline{x} - \tilde{\underline{x}}) + \frac{1}{2!} (\underline{x} - \tilde{\underline{x}})^T g_i''(\tilde{\underline{x}}) (\underline{x} - \tilde{\underline{x}}) + \dots - h_i = 0 \quad (12)$$

where the superscripts ' and '' denote the first and second partial derivatives.

Keeping only the first-order terms, some rearrangement leads to

$$g'(\tilde{\underline{x}})^T \underline{x} \approx \underline{h} - g(\tilde{\underline{x}}) + g'(\tilde{\underline{x}})^T \tilde{\underline{x}} \quad (13)$$

where $g(\underline{x}) = [\dots g_i(\underline{x}) \dots]^T$, $\underline{d} = [\dots d_i \dots]^T$, and $g'(\underline{x}) = [\dots g_i'(\underline{x}) \dots]$. An approximate linear constraint is therefore formed by replacing D and \underline{d} in (3) with $g'(\underline{x})^T$ and $\underline{h} - g(\tilde{\underline{x}}) + g'(\tilde{\underline{x}})^T \tilde{\underline{x}}$, respectively.

Fig. 1 illustrates this linearization process and identifies possible errors associated with linear approximation of a nonlinear state constraint. As shown, the previous constrained state estimate $\tilde{\underline{x}}^-$ lies somewhere on the constrained surface but is away from the true state \underline{x} . The projection of the unconstrained state estimate $\hat{\underline{x}}$ onto the approximate linear state constraint produces the current constrained state estimate $\tilde{\underline{x}}^+$, which is however subject to the constraint approximation error. Clearly, the further away $\tilde{\underline{x}}^-$ is from \underline{x} , the larger error is the approximation introduced. More critically, such an approximately linear constrained estimate may not satisfy the original nonlinear constraint specified in (25). It is therefore desired to reduce this approximation-introduced error by including higher-order terms while keeping the problem computationally tractable. One possible approach is presented in the next section.

Iterative Solution to Second-Order Constraints

Naturally formed roads tend to have more bends and turns of irregular shapes (high nonlinearity). Even highways have to follow terrain contours when crossing mountains. Locally, however, it suffices to represent a curved road segment by a second-order state constraint function as

$$f(\underline{x}) = \begin{bmatrix} \underline{x}^T & 1 \end{bmatrix} \begin{bmatrix} M & \underline{m} \\ \underline{m}^T & m_0 \end{bmatrix} \begin{bmatrix} \underline{x} \\ 1 \end{bmatrix} = \underline{x}^T M \underline{x} + \underline{m}^T \underline{x} + \underline{x}^T \underline{m} + m_0 = 0 \quad (14)$$

which can be viewed as a second-order approximation to an arbitrary nonlinearity in a digital terrain map.

Similar to (4), we can formulate the projection of an unconstrained state estimation onto a nonlinear constraint surface as the constrained least-square optimization problem

$$\hat{\underline{x}} = \arg \min_{\underline{x}} (\underline{z} - H \underline{x})^T (\underline{z} - H \underline{x}) \quad (15a)$$

$$\text{subject to } g(\underline{x}) = 0 \quad (15b)$$

If we let $W = H^T H$ and $z = H \hat{\underline{x}}$, the formulation in (15) becomes the same as in (4). In a sense, (15) is a more general formulation because it can also be interpreted as a

nonlinear constrained measurement update or a projection in the predicted measurement domain.

The solution to the constrained optimization (15) can be obtained again using the Lagrangian multiplier technique as

$$\hat{\underline{x}} = G^{-1}V(I + \lambda\Sigma^T\Sigma)^{-1}\underline{e}(\lambda) \quad (16a)$$

$$q(\lambda) = \sum_i \frac{e_i^2(\lambda)\sigma_i^2}{(1 + \lambda\sigma_i^2)^2} + 2\sum_i \frac{e_i(\lambda)t_i}{1 + \lambda\sigma_i^2} + m_0 = 0 \quad (16b)$$

where G is an upper right diagonal matrix resulting from the Cholesky factorization of $W = H^T H$ as

$$W (= H^T H) = G^T G \quad (16c)$$

V , an orthonormal matrix, and Σ , a diagonal matrix with its diagonal elements denoted by σ_i , are obtained from the singular value decomposition (SVD) of the matrix LG^{-1} as

$$LG^{-1} = U\Sigma V^T \quad (16d)$$

where U is the other orthonormal matrix of the SVD and L results from the factorization $M = L^T L$, and

$$\underline{e}(\lambda) = [\dots e_i(\lambda), \dots]^T = V^T(G^T)^{-1}(H^T \underline{z} - \lambda \underline{m}) \quad (16e)$$

$$\underline{t} = [\dots t_i \dots]^T = V^T(G^T)^{-1} \underline{m} \quad (16f)$$

As a nonlinear equation in λ , it is difficult to find a closed-form solution in general for the nonlinear equation $q(\lambda) = 0$ in (16b). Numerical root-finding algorithms may be used instead. For example, the Newton's method is used below. Denote the derivative of $q(\lambda)$ with respect to λ as

$$\begin{aligned} \dot{q}(\lambda) = & 2\sum_i \frac{e_i(\lambda)\dot{e}_i(1 + \lambda\sigma_i^2)\sigma_i^2 - e_i^2(\lambda)\sigma_i^4}{(1 + \lambda\sigma_i^2)^3} \\ & + 2\sum_i \frac{\dot{e}_i t_i (1 + \lambda\sigma_i^2) - e_i(\lambda)t_i \sigma_i^2}{(1 + \lambda\sigma_i^2)^2} \end{aligned} \quad (17a)$$

where

$$\dot{\underline{e}} = [\dots \dot{e}_i \dots]^T = -V^T(G^T)^{-1} \underline{m} \quad (17b)$$

Then the iterative solution for λ is given by

$$\lambda_{k+1} = \lambda_k - \frac{q(\lambda_k)}{\dot{q}(\lambda_k)}, \quad \text{starting with } \lambda_0 = 0 \quad (18)$$

The iteration stops when $|\lambda_{k+1} - \lambda_k| < \tau$, a given small value or the number of iterations reaches a pre-specified number. Then bringing the converged Lagrangian multiplier λ back to (16a) provides the constrained optimal solution.

Now consider the special case where $W = H^T H$, $\underline{z} = H \hat{\underline{x}}$, and $\underline{m} = 0$, that is, a quadratic constraint on the state. Under these conditions, $\underline{t} = 0$ and \underline{e} is no longer a function

of λ so its derivative relative to λ vanishes, $\dot{\underline{e}} = 0$. The quadratic constrained solution is then given by

$$\tilde{\underline{x}} = (W + \lambda M)^{-1} W \hat{\underline{x}} \quad (19a)$$

where the Lagrangian multiplier λ is obtained iteratively as in (18) with the corresponding $q(\lambda)$ and $\dot{q}(\lambda)$ given by

$$q(\lambda) = \sum_i \frac{e_i^2 \sigma_i^2}{(1 + \lambda \sigma_i^2)^2} + m_0 = 0 \quad (19b)$$

$$\dot{q}(\lambda) = -2 \sum_i \frac{e_i^2 \sigma_i^4}{(1 + \lambda \sigma_i^2)^3} \quad (19c)$$

The solution of (19) is also called the constrained least squares [Moon and Stirling, 2000: pp 765-766], which was previously applied for the joint estimation and calibration [Yang and Lin, 2004]. Similar techniques have been used for the design of filters for radar applications [Abramovich and Sverdluk, 1970] and in robust minimum variance beamforming [Lorenz and Boyd, 2006]. When $M = 0$, the constraint in (14) degenerates to a linear one. The constrained solution is still valid. However, the iterative solution for finding λ is no longer applicable but a closed-form solution is available instead as given in (5).

Geometric Interpolation for Simple Cases

Consider a simple example where a target travels along a circle. For this case, in fact, a closed-form solution can be derived. Assume that $W = I_2$, $M = I_2$, $\underline{m} = 0$, and $m_0 = -r^2$. The nonlinear constraint can be equivalently written as

$$\underline{x}^T \underline{x} = r^2 \quad (20)$$

The quadratic constrained estimate given in (19a) becomes

$$\tilde{\underline{x}} = (W + \lambda M)^{-1} W \hat{\underline{x}} = (1 + \lambda)^{-1} \hat{\underline{x}} \quad (21)$$

where λ is the Lagrangian multiplier.

Bringing (21) back to (20) gives

$$\tilde{\underline{x}}^T \tilde{\underline{x}} = \left(\frac{\hat{\underline{x}}}{1 + \lambda}\right)^T \frac{\hat{\underline{x}}}{1 + \lambda} = r^2 \quad (22)$$

The solution for λ is

$$\lambda = \frac{\sqrt{\hat{\underline{x}}^T \hat{\underline{x}}}}{r} - 1 = \frac{\|\hat{\underline{x}}\|_2}{r} - 1 \quad (23)$$

where $\|\cdot\|_2$ stands for the 2-norm or length for the vector.

Bringing the solution for λ in (23) back to (21) gives

$$\tilde{\underline{x}} = r \frac{\hat{\underline{x}}}{\|\hat{\underline{x}}\|_2} \quad (24)$$

This indicates that for this particular case with a circular constraint, the constraining results in normalization.

This further suggests a simple solution for some practical applications. When a vehicle is traveling along a circular path (or approximately so), one can first find the equivalent center of the circle around which to establish a new coordinate system, then express the unconstrained solution in the new coordinate and normalize it as the constrained solution. This solution can then be converted back to the original coordinates. For non-circular but second-order paths, eigenvalue-based scaling may be effected following coordinate translation and rotation in order to apply this circular normalization. Reverse operations are then used to transform back. For applications of high dimensionality, the scalar iterative solution of (17) may be more efficient.

SIMULATION RESULTS

The simulation presented in this section is adapted from [Yang and Blasch, 2006b]. More results can be found in [Yang and Blasch, 2006a; 2006b]. In this example, a ground vehicle is assumed to travel along a circular road segment as shown in Fig. 1. The turn center is chosen as the origin of the x-y coordinates and the turn radius is $r = 100$ m. The vehicle maintains a constant turn rate of 5.7 deg/s with an equivalent linear speed of 10 m/s. The initial state is

$$\underline{x}_{k=0} = [x \quad \dot{x} \quad y \quad \dot{y}]^T = [100 \text{ m}, 0 \text{ m/s}, 0 \text{ m}, 10 \text{ m/s}]^T \quad (25)$$

The GPS fixes of the vehicle are available at a sampling interval of $T = 1$ s, which can be modeled as position measurements of the vehicle as

$$\underline{y}_k = \begin{bmatrix} 1 & 0 & 0 & 0 \\ 0 & 0 & 1 & 0 \end{bmatrix} \underline{x}_k + \underline{v}_k \quad (26)$$

where the measurement error $\underline{v} \sim \mathcal{N}(\underline{0}, R)$ is a zero-mean Gaussian noise, independent in the x- and y-axis. The covariance matrix $R = \text{diag}([\sigma_{rx}^2 \quad \sigma_{ry}^2])$ uses the particular values of $\sigma_{rx} = \sigma_{ry} = 7$ m in the simulation.

For a loosely coupled integration, a simple discrete-time second-order kinematic model is used by the integration Kalman filter

$$\underline{x}_{k+1} = \begin{bmatrix} 1 & T & 0 & 0 \\ 0 & 1 & 0 & 0 \\ 0 & 0 & 1 & T \\ 0 & 0 & 0 & 1 \end{bmatrix} \underline{x}_k + \begin{bmatrix} \frac{1}{2}T^2 & 0 \\ T & 0 \\ 0 & \frac{1}{2}T^2 \\ 0 & T \end{bmatrix} \underline{w}_k \quad (27)$$

where the process noise $\underline{w} \sim \mathcal{N}(\underline{0}, Q)$ is also a zero-mean Gaussian noise, independent of the measurement noise \underline{v} . The covariance matrix $Q = \text{diag}([\sigma_{\dot{x}}^2 \quad \sigma_{\dot{y}}^2])$ uses the particular values of $\sigma_{\dot{x}} = \sigma_{\dot{y}} = 0.32 \text{ m/s}^2$ in the simulation. The GPS fixes in (40) are assumed to be obtained inside a GPS receiver either by a nonlinear least square method or by an extended Kalman filter. In the

latter case, a cascaded two Kalman filters is implied, one for the GPS receiver and the other for the integration filter.

When represented in a Cartesian coordinate system, a vehicle traveling along a curved road is certainly subject to acceleration in both the x- and y-axis. However, no effort was made in this simulation to optimize the integration filter for maneuver but merely selecting Q and the initial conditions so as to focus on constraining the estimates. The initial state is selected to be the same as the true state, i.e., $\hat{\underline{x}}_0 = \underline{x}_0$ and the initial estimation error covariance is selected to be

$$P_0 = \text{diag}([5^2 \quad 1^2 \quad 5^2 \quad 1^2]) \quad (28)$$

Fig. 2 shows sample trajectories of the linear constrained Kalman filter. There are 5 curves and 2 series of data points in the figure. The true state is represented by a series of dots (\cdot) at consecutive sampling instants, which is plotted on the solid line being the road segment. The corresponding measurements are a series of circles (\circ).

The estimates of the unconstrained Kalman filter are shown as the connected triangles (Δ) whereas those of linearly constrained Kalman filters are shown as the connected crosses (\times), stars (*), and pluses (+) for three linear approximations of the nonlinear constraint of curved road, respectively.

In the first approximation (the line with cross \times labeled “linear constraint 1”), a single linearizing point at $\theta_1 = 10^\circ$ is chosen to cover the entire curved road, where θ is the angle made relative to the x-axis, positive in the counter-clock direction. The linearized state constraint at θ_1 can be written as

$$\begin{bmatrix} \cos \theta_1 & 0 & \sin \theta_1 & 0 \\ 0 & \cos \theta_1 & 0 & \sin \theta_1 \end{bmatrix} \underline{x} = \begin{bmatrix} r \\ 0 \end{bmatrix} \quad (29)$$

Although all estimates are faithfully projected by the constrained filter onto this linear constraint, tangential to the curve at the linearizing point, it runs away from the true trajectory and the resulting errors continue to grow. The apparent divergence is caused by the choice of linearization.

In the second approximation (the line with star * labeled “linear constraint 2”), two linearizing points at $\theta_1 = 15^\circ$ and $\theta_2 = 80^\circ$ are chosen to cover the curved road with two linear segments. The switching point from one linear segment to the other in this case is at $\theta = 45^\circ$. As shown, the estimates are projected onto one of the two linear segments. Except near the corner where the two linear approximations intersect (which is far away from both linearizing points), the linear constrained estimates typically outperform the unconstrained estimates (closer to the true state). This is better illustrated in Fig. 3 where

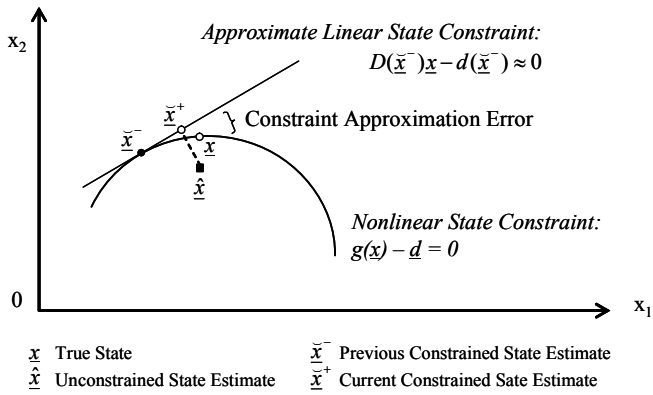


Fig. 1. Errors in Linear Approximation of Nonlinear State Constraints

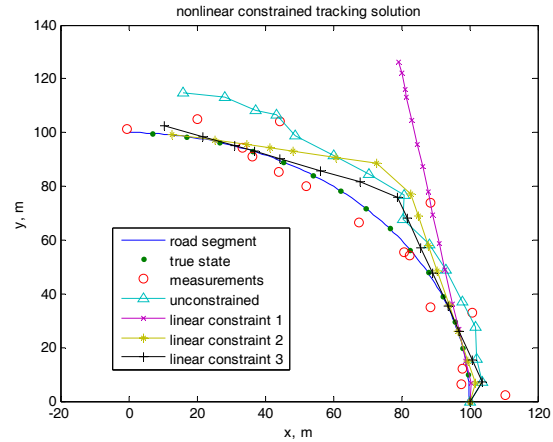


Fig. 2. Sample Trajectories for Linear Constrained Kalman Filter

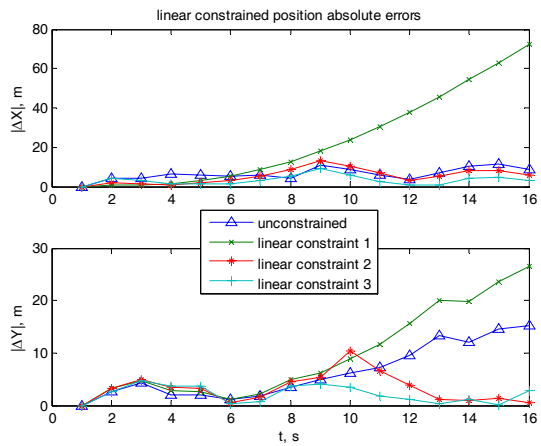


Fig. 3. Linear Constrained Position Errors vs. Time

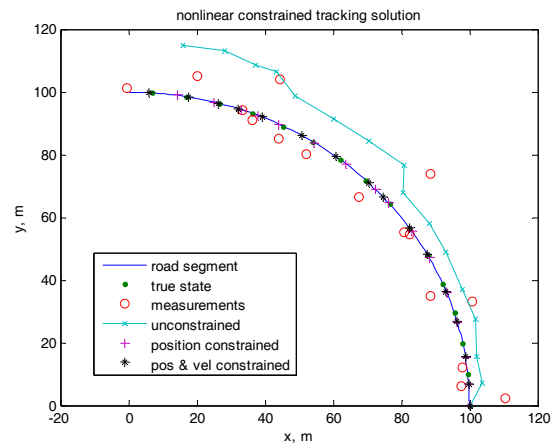


Fig. 4. Sample Trajectories for Nonlinear Constrained Kalman Filter

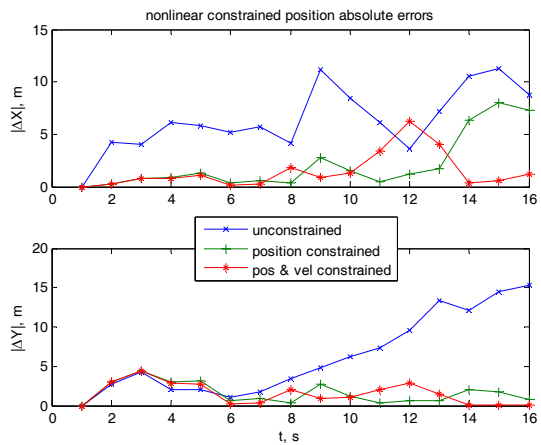


Fig. 5. Nonlinear Constrained Position Errors vs. Time

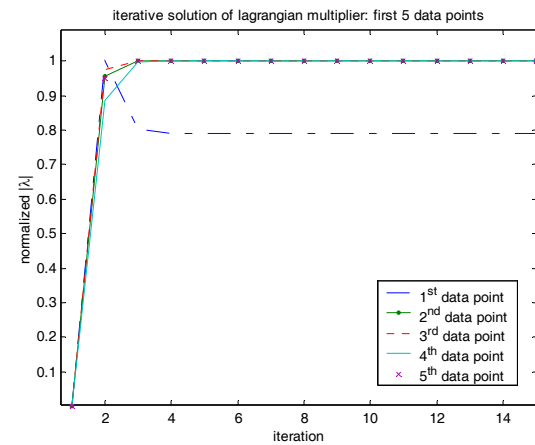


Fig. 6. Convergence in Iterative Lagrangian Multiplier

the upper plot is for the absolute position error in x while the lower plot is for the absolute position error in y , both plotted as a function of time.

Still with two linearizing points and the same switching point at $\theta = 45^\circ$, the third approximation (the line with star + labeled “linear constraint 3”) adjusts linearizing points to $\theta_1 = 20^\circ$ and $\theta_2 = 70^\circ$. A better overall performance is achieved as shown in Fig. 3.

It is clear from Fig. 2 that a nonlinear constraint can be approximated with linear constraints in a piecewise fashion. By judicious selection of the number of linear segments and their placement (*i.e.*, the point around which to linearize), a reasonably good performance can be expected. In the limit, a nonlinear function is represented by a piecewise function composed of an infinite number of linear segments. This naturally leads to the use of nonlinear constraints.

Fig. 4 shows sample trajectories of the nonlinear constrained Kalman filter. There are 2 curves and 3 series of data points in the figure. The true state is still represented by a series of dots (\cdot) at the sampling instants, which is plotted on the solid line of road segment. The corresponding measurements are again a series of circles (\circ). The unconstrained Kalman filter is shown as the connected crosses (\times) whereas the estimates of nonlinearly constrained Kalman filters are shown as a series of connected pluses (+) and stars (*) for two implementations, respectively.

The first implementation (the series of pluses +) only applies the nonlinear constraint to the position estimate whereas the second implementation (the series of stars *) applies constraints to both the position and velocity estimates. In fact, we encounter a hybrid (mixed) linear and nonlinear state constraint situation. The constrained position estimate is given by (19) for the quadratic case (equivalent to (24) for a circular road). Since the velocity direction is along the tangent of the road curve, the constrained velocity estimate is obtained by the following projection

$$\hat{\underline{v}}_{constrained} = (\hat{\underline{v}}_{unconstrained} \underline{\mu}) \underline{\mu} \quad (30)$$

where $\hat{\underline{v}} = \begin{bmatrix} \hat{x} & \hat{y} \end{bmatrix}^T$ is the estimated velocity vector and $\underline{\mu} = [-\sin\theta \quad \cos\theta]^T$ is the constrained unit direction vector associated with the constrained position at $\theta = \tan^{-1}(\hat{y} / \hat{x})$.

For simplicity, the unconstrained estimation error covariance is not modified in the present simulation after the constrained estimate is obtained using the projection algorithms in (19) and (30). The implementation is therefore pessimistic (suboptimal) in the sense that it does not take into account the reduction in the estimation error covariance brought in by constraining. One consequence

of this simplification is more volatile state estimates. To quantify this effect, one approach is to project the unconstrained probability density function (*i.e.*, a normal distribution with support on the whole state space) onto the nonlinear constraint. Statistics can then be calculated from the constrained probability density function with the constraint as its support. Again, the resulting error ellipse represented by the covariance matrix is only an approximation to the second order.

As shown in Fig. 4, both the nonlinear constrained estimates fall onto the road as expected. Overall the position and velocity constrained estimates are better (closer to the true state) than the position-only constrained estimates. This is illustrated in Fig. 5 where the upper plot is for the absolute position error in x while the lower plot is for the absolute position error in y .

A Monte Carlo simulation is used to generate the RMS errors of state estimation. The results are based on a total of 100 runs across 16 updates and summarized in Table I. The performance improvement of the nonlinear constrained filter over the linearized constrained filter is demonstrated.

Finally, we use Fig. 6 to show an example of the Lagrangian multiplier as it is calculated iteratively using (19). The runs for five unconstrained state estimates are plotted in the same figure and to make it fit, the normalized absolute values of λ are taken. As shown, starting from zero, it typically takes 4 iterations for the algorithm to converge in the example presented.

Table I. RMS Estimation Errors

Estimators	RMS Estimation Error	
	Position (m)	Velocity (m/s)
Unconstrained	8.3663	4.2640
Best Linear Constrained	5.5386	2.5466
Nonlinear Constrained	1.8056	0.4252

CONCLUSIONS

In this paper, we presented an approach to incorporating road information into navigation solution via GPS/map integration. In this approach, road segments were modeled with analytic functions and their fusion with a position fix was cast as a linearly or nonlinearly state constrained optimization procedure. With the Lagrangian multiplier, a closed-form solution was found for linear constraints and an iterative solution for nonlinear constraints. Geometric interpretations of the solutions were provided for simple cases. Computer simulation results demonstrate the performance of the algorithms.

Future work includes both algorithms development and practical applications. It is of interest to extend the

iterative method presented in the paper for second-order nonlinear state constraints to other types of nonlinear constraints of practical significance and to search for more efficient root-finding algorithms to solve for the Lagrangian multiplier. Similarly, the simple fusion to a single road as presented in this paper is being extended to an urban environment with a vehicle moving along closely-spaced road networks with intersections and by-passes. In this case, the fusion (or constraining) can take place in the measurement level as well as in the position level, involving road constrained data association (RCDA) and map-predictive model selection and updating. Results will be reported in future papers.

ACKNOWLEDGEMENTS

Research supported in part under Contracts No. FA8650-05-C-1808 and FA8650-05-C-1828, which is gratefully acknowledged.

REFERENCES

- Abromovich, Y.I. and Sverdlik, M.B., Synthesis of a Filter Response Which Maximizes the Signal to Noise Ratio under Additional Quadratic Constraints, *Radio Eng. and Electron. Phys.*, **5** (Nov. 1970), 1977-1984.
- Anderson, B. and Moore, J., *Optimal Filtering*, Englewood Cliffs, NJ: Prentice Hall, 1979.
- Bar-Shalom, Y. and Li, X.R., *Multitarget-Multisensor Tracking: Principles and Techniques*, Storrs, CT: YBS Publishing, 1995.
- Blackman, S. and R. Popoli, *Design and Analysis of Modern Tracking Systems*, Boston, MA: Artech House, 1999.
- Bullock, J.B., M. Foss, G.J. Geier, and M. King, "Integration of GPS with Other Sensors and Network Assistance," in *Understanding GPS: Principles and Applications*, E.D. Kaplan and C.J. Hegarty (Eds.), Artech House, Boston, MA, 2006.
- Kirubarajan, T., Bar-Shalom, Y., Pattipati, K.R., and Kadar, I., Ground Target Tracking with Variable Structure IMM Estimator, *IEEE Trans. On Aerospace and Electronic Systems*, **36** (Jan. 2002), 26-46.
- Lorenz, R.G. and Boyd, S.P., Robust Minimum Variance Beamforming, in *Robust Adaptive Beamforming*, J. Li and P. Stoica (Eds.), Hoboken, NJ: Wiley-Interscience, 2006.
- Moon, T.K. and Stirling, W.C., *Mathematical Methods and Algorithms for Signal Processing*, Upper Saddle River, NJ: Prentice Hall, 2000.
- Ristic, B., Arullampalam, S. and Gordon, N., *Beyond the Kalman Filter – Particle Filters for Tracking Applications*, Boston, MA: Artech House, 2004.
- Simon, D. and Chia, T.L., Kalman Filtering with State Equality Constraints, *IEEE Trans. On Aerospace and Electronic Systems*, **38** (Jan. 2002), 128-136.
- Yang, C., Bakich, M., and Blasch, E., Nonlinear Constrained Tracking of Targets on Roads, in *Proc. of the 8th International Conf. on Information Fusion*, Philadelphia, PA, July 2005.
- Yang, C. and Blasch, E., Kalman Filtering with Nonlinear State Constraints, In *Proc. of the 9th International Conf. on Information Fusion*, Florence, Italy, July 2006a.
- Yang, C. and Blasch, E., Track Fusion with Road as Nonlinear Constraints, Submitted for Publication to *ISIF Journal of Advanced Information Fusion*, August 2006b.
- Yang, C. and Lin, D.M., Constrained Optimization for Joint Estimation of Channel Biases and Angles of Arrival for Small GPS Antenna Arrays, in *Proc. of the 60th Annual Meeting of the Institute of Navigation*, Dayton, OH, June 2004, 548-559.